Received: 28 July 2016 | Revised: 31 July 2017 | Accepted: 17 September 2017

DOI: 10.1002/ldr.2832

WILEY

SPECIAL ISSUE ARTICLE

Effects of vegetation rehabilitation on soil organic and inorganic carbon stocks in the Mu Us Desert, northwest China

Yang Gao[1,2] | Peng Dang[2] | Qingxia Zhao[2] | Jinliang Liu[2] | Jiabin Liu[3]

[1] State Key Laboratory of Soil Erosion and Dryland Farming on the Loess Plateau, Northwest A&F University, Yangling 712100, Shaanxi, PR China

[2] College of Forestry, Northwest A&F University, Yangling 712100, Shaanxi, PR China

[3] College of Natural Resources and Environment, Northwest A&F University, Yangling 712100, Shaanxi, PR China

Correspondence
J. Liu, College of Natural Resources and Environment, Northwest A&F University, No. 3 Taicheng Road, Yangling District, 712100, Shaanxi, PR China.
Email: liujb@nwsuaf.edu.cn

Funding information
National Natural Science Foundation of China, Grant/Award Number: 31500585

Abstract

In arid and semiarid areas, the importance of soil inorganic carbon (SIC) is at least as high as that of soil organic carbon (SOC) in affecting the regional carbon budget following vegetation rehabilitation. However, variations in SIC have been uncertain, and few studies have analyzed the interactions between the SOC and SIC pools. We measured SIC, SOC, δ^{13}C-SIC, and δ^{13}C-SOC after planting Mongolian pine (MP) and *Artemisia ordosica* (AO) on shifting sand land (SL) over 10 years in the Mu Us Desert, northwest China. The results showed that, compared to SL, SIC stocks at 0–100 cm in MP and AO lands significantly increased by 12.6 and 25.8 Mg ha^{-1}, respectively; SOC stocks in MP and AO lands significantly increased by 24.0 and 38.4 Mg ha^{-1}, respectively. Both δ^{13}C-SIC and δ^{13}C-SOC in the 2 plantation lands were significantly lower than those in SL were. All 315 samples exhibited a negatively linear relationship between SIC content and δ^{13}C-SIC (R^2 = .70, p < .01) and showed positively linear relationships between SIC content and SOC content (R^2 = .69, p < .01) and between δ^{13}C-SIC and δ^{13}C-SOC (R^2 = .61, p < .01). The results demonstrated that vegetation rehabilitation on SL has a high potential to sequester SIC and SOC in semiarid deserts. The reduction in δ^{13}C-SIC and the relationship of SIC with δ^{13}C-SIC following vegetation rehabilitation suggested that SIC sequestration is likely caused by the formation of pedogenic inorganic carbon. The relationships between SIC and SOC and between δ^{13}C-SIC and δ^{13}C-SOC implied that the pedogenic inorganic carbon formation may be closely related to the SOC accumulation.

KEYWORDS

desert, shifting sand land, soil inorganic carbon, stable carbon isotope, vegetation rehabilitation

1 | INTRODUCTION

Land degradation is the most challenging environmental problem in drylands (Easdale, 2016). In the past decades, over two thirds of arid and semiarid areas have experienced desertification, leading to 19–29 Pg (10^{15} g) of soil carbon loss (Lal, 2004; Li et al., 2015). If appropriate restoration measures were successfully implemented on the degraded lands, these lands could potentially sequester a large amount (12–18 Pg) of carbon in the soil (Huang, Zhao, Li, & Cui, 2012; Lal, 2009). As an important restoration measure, vegetation rehabilitation on degraded land, including the planting of drought-tolerant trees and shrubs, can combat desertification, improve soil properties, and alter soil carbon pool (Chen, Duan, & Tan, 2016; Su, Wang, Yang, & Lee, 2010; Zhao et al., 2007). The soil carbon pool is comprised of soil organic carbon (SOC) and soil inorganic carbon (SIC) pools. Due to its potentially rapid response to land use changes, the SOC pool has received considerable attention and has been extensively investigated. Notably, vegetation rehabilitation can induce SOC sequestration with substantial organic litter being introduced into the soil (Chaplot, Dlamini, & Chivenge, 2016; Novara, Gristina, Mantia, & Rühl, 2013), and the accumulation rate ranges from 0 to 0.2 Mg ha^{-1} yr^{-1} in semiarid areas (Lal, 2009; Zhang, Dang, Tan, Cheng, & Zhang, 2010). Unlike the attention given to SOC, SIC dynamics following vegetation rehabilitation have been seldom studied. However, the importance of SIC is at least as high as that of SOC in affecting regional carbon budget following vegetation rehabilitation (Zamanian, Pustovoytov, & Kuzyakov, 2016). SIC is the dominant form of carbon in arid and semiarid areas, and its content in first 2 m of soil in these regions could be 10 or even up to 17-times higher than that of SOC (Diaz-Hernández, Fernández, & González, 2003; Emmerich, 2003). Due to the absolute predominance of SIC in the whole soil carbon pool, a subtle change in SIC pool may have a more significant

impact than a considerable fluctuation of SOC pool in altering carbon budget in semiarid areas. Therefore, the dynamics of the SIC pool following vegetation rehabilitation should be well understood in such regions (Jin et al., 2014; Landi, Mermut, & Anderson, 2003).

Changes in SIC following vegetation rehabilitation are highly uncertain in arid and semiarid areas. For instance, in the Badain Jaran Desert, China, the SIC concentration at 0–15 cm increased by 45.7% after afforestation with poplar on sand land (SL) over 7 years (Su et al., 2010). However, in the desert of the Columbia Plateau, Oregon, USA, 10 years of poplar planting reduced the SIC concentration from 2.6 to 1.2 g kg^{-1} in the surface layer (0–10 cm; Sartori, Lal, Ebinger, & Eaton, 2007). In the Chinese Loess Plateau, Wang et al. (2016) reported that the SIC storage at depth of 0–100 cm in a farmland area was significantly lower than that in an area of restored artificial forestland, with a difference of 16.8 Mg ha^{-1}. Nevertheless, also in this region, Chang, Fu, Liu, Wang, and Yao (2012) noted that afforestation in farmland areas only redistributed SIC throughout the soil profile without affecting the total SIC stock of the layer of 0–100 cm. Under similar climate, soil type, applied species, and plantation age conditions, the SIC dynamics following vegetation rehabilitation can exhibit various and even contradictory trends; therefore, the variations in SIC following vegetation rehabilitation in arid and semiarid areas must be urgently studied.

Moreover, uncertainty nonetheless remains as to why SIC pool showed variations following vegetation rehabilitation. The SIC pool is composed of two subpools with different $\delta^{13}C$ values: the lithogenic inorganic carbon (LIC) subpool and the pedogenic inorganic carbon (PIC) subpool (Chang et al., 2012; Tan et al., 2014). LIC is inherited from parent material, and its $\delta^{13}C$ value is close to zero. PIC is generated from carbonate precipitation, and its $\delta^{13}C$ value is negative (Meyer, Breecker, Young, & Litvak, 2014; Zamanian et al., 2016). Various processes that lead to SIC variations, including the mixing of LIC and PIC and the reaction of soil carbonate with biogenic CO_2, are sensitively and precisely reflected by $\delta^{13}C$ values (Monger et al., 2015; Stevenson, Kelly, McDonald, & Busacca, 2005). The use of stable soil carbon isotopes method, in which the soil inorganic $\delta^{13}C$ value ($\delta^{13}C$-SIC) and the soil organic $\delta^{13}C$ value ($\delta^{13}C$-SOC) are measured, has been found to be an ideal approach for studying the inherent mechanisms of SIC dissolution, sequestration, and transformation following land use changes (Bughio et al., 2016; Stevenson et al., 2005; Wang, Wang, Xu, et al., 2015). However, the existing methods of carbon isotope analysis have not been extensively utilized to explore the reasons for SIC variations following vegetation rehabilitation, particularly in semiarid deserts.

To control the expansion of desertification, a series of restoration efforts have been implemented on shifting SL in northern China. Vegetation rehabilitation by planting Mongolian pine (*Pinus sylvestris* var. *mongolica* Litv. [MP]) and *Artemisia ordosica* (AO) have been regarded as the successful measures for mobile sand dune restoration (Li et al., 2012; Zhang, Cao, Han, & Jiang, 2013). Numerous studies have demonstrated that vegetation rehabilitation on SL can remarkably elevate SOC stock by several to ten times (Li et al., 2013; Su et al., 2010; Yu & Jia, 2014; Zhang, Cao, et al., 2013; Zhao et al., 2007). The SOC accumulation can dramatically elevate soil respiration and soil CO_2 concentration (Zhang, Li, et al., 2013). In soils of arid and semiarid regions, which usually have high pH (>8.5) and rich Ca^{2+} and/or Mg^{2+} (>0.1%; Zamanian et al., 2016), the respired CO_2 combined with the available cations may promote the formation of PIC and lead to SIC sequestration (Meyer et al., 2014; Wang, Wang, Zhang, & Zhao, 2015). The $\delta^{13}C$ of the newly formed PIC is much lower than the $\delta^{13}C$-LIC (−2‰ to 2‰; Marion, Introne, & Cleve, 1991; Ryskov, Demkin, Oleynik, & Ryskova, 2008), as the $\delta^{13}C$ of respired CO_2 is generally below −20‰ (Cerling, 1984). The mixing of LIC and new formed PIC will inevitably reduce the $\delta^{13}C$ of the whole carbonate ($\delta^{13}C$-SIC; Stevenson et al., 2005; Zamanian et al., 2016). Therefore, the PIC formation induced by SOC accumulation can be clearly reflected by the stable carbon isotopes. On the basis of the changes in $\delta^{13}C$-SIC and $\delta^{13}C$-SOC in arid and semiarid croplands, straw organic amendments and applying organic fertilizers were found to enhance PIC formation and lead to SIC accumulation in the rates of 101–380 g m^{-2} yr^{-1} (Bughio et al., 2016; Wang et al., 2014). Similar to fertilization with organic matter in cropland, vegetation rehabilitation on SL also introduces organic litter into soil, and it may alter the SIC stock. However, few studies have analyzed the interactions between the SOC and SIC pools using stable carbon isotopes, although Lal (2001) proposed that SIC stock could be enhanced by vegetation rehabilitation in desert ecosystems. In this study, we hypothesized that vegetation rehabilitation could induce SIC sequestration in a semiarid desert. To test this hypothesis, we conducted a research after planting MP and AO over 10 years on SL in the Mu Us Desert, northwest China. We measured SIC, SOC, $\delta^{13}C$-SOC, and $\delta^{13}C$-SIC in SL, forestland, and shrubland at a depth of 100 cm. The objectives of this research were (a) to examine the changes in SIC following vegetation rehabilitation on SL, (b) to explore the reasons for SIC variation on the basis of the stable carbon isotopes, and (c) to analyze the effects of the SOC accumulation on SIC pool. This information is considerably meaningful and necessary for precisely assessing the carbon budget in desert areas.

2 | MATERIALS AND METHODS

2.1 | Study site description

The study site is located at the Yanchi Research Station, Ningxia Province, China (37°42′N, 107°13′E), on the southwestern edge of the Mu Us Desert. The region has a typical temperate continental monsoon climate at an elevation of 1,540 m. The mean annual precipitation is 275 mm with 73% occurring in summer and autumn. The mean annual temperature is 7 °C. The average relative humidity is 51%, and the frost-free period lasts 128 days. The soil is characterized by Cambic Arenosols (FAO, 2006) with a pH ranging from 8.4 to 8.6 and less than 10% fine particles (<0.05 mm). Before vegetation rehabilitation, the landscape of the research area was covered by SL, which was composed of many connected and active sand dunes without vegetation. The research station had been established since the 1990s. At the beginning of the 2000s, vegetation rehabilitation with MP and AO on SL was simultaneously performed at the station to combat the shifting sand and to protect the buildings. Currently, the movement of SL surrounding the buildings (radius of 1–3 km) has been stabilized by MP and AO, and no soil erosion has occurred in this site. Outside the plantation area, many sand dunes remain active. Within the 2 km × 2 km

scope of the study site, we selected a forestland, a shrubland, and a connected SL as our three treatments: (a) 10-year-old MP land, (b) 10-year-old AO land, and (c) SL (Figure 1). Within each treatment, we selected one sample plot. The distribution of the three sample plots in the study site was illustrated in Figure 1, and sample plot information, including soil properties, was shown in Table 1.

2.2 | Soil sampling

Twenty-one subplots of 15 m × 15 m were randomly selected within each sample plot for soil sampling. Soil was sampled from an S-shaped curve in each subplot. Soil samples were obtained at a depth interval of 20 cm from 0 to 100 cm using a soil auger (10 cm in diameter) after removing litter. Five soil samples obtained from the same layer in each subplot were mixed into a composite sample. One hundred five composite samples from the 21 subplots within each sample plot were obtained. After all 315 composite samples from the three sample plots were air-dried, roots were removed, and each composite sample was split into three subsamples of 150 g each. One subsample was ground and sieved to <0.075 mm for total soil carbon (TSC) analysis; one subsample was ground and sieved to <0.1 mm for SOC analysis; and the final subsample was ground and sieved to <0.05 mm for $\delta^{13}C$ analysis.

After obtaining the 315 composite samples, nine subplots were randomly selected from the above 21 subplots within each sample plot for measuring bulk density. For the nine subplots, a soil profile from 0 to 100 cm was excavated in each subplot. A metal corer (100 cm^3 in volume) was driven into the soil at a depth interval of 20 cm from 0 to 100 cm, and soil samples were oven dried at 115 °C for 24 hr and weighed to determine the bulk density. From each excavated soil profile, additional five soil samples (approximately 100 g for each) were obtained at a depth interval of 20 cm from 0 to 100 cm to measure the particle size distribution using a particle size analyzer (Malvern Laser Mastersizer 2000, England).

2.3 | Soil analyses

The TSC content was measured using a Vario EL III elemental analyzer (Elementar, Germany). The SOC content was determined using the dichromate oxidation procedure described by Walkley and Black (1934). The SOC content was subtracted from the TSC content to obtain the precise SIC content (Li et al., 2013).

The stocks of SIC and SOC were calculated as follows:

$$M = 0.1 \times D \times B \times Z \times ((100 - G)/100), \quad (1)$$

Where: M is the soil carbon stock per unit area (Mg ha^{-1}); D is soil depth (cm); B is the bulk density (g cm^{-3}); Z is the carbon content (g kg^{-1}); and G is the relative amount of gravel (%). The gravel content was 0% because there was no gravel in the soil.

The $\delta^{13}C$-SOC and $\delta^{13}C$-SIC have been applied successfully in analyzing the mechanisms of SIC variation in agro-ecosystem and forest ecosystem in the arid and semiarid regions (Bughio et al., 2016; Jin et al., 2014; Wang et al., 2014). The methods for determining $\delta^{13}C$-SOC and $\delta^{13}C$-SIC are highly reliable at present. In this study, the pretreatments for determining $\delta^{13}C$-SOC and $\delta^{13}C$-SIC were the same as in Jin et al. (2014). After the pretreatments, the detailed operations for measuring $\delta^{13}C$ values with isotope ratio mass spectrometer (IRMS) were consistent with the normalization procedure of International Union of Pure and Applied Chemistry guidelines (Coplen, 2011). To determine $\delta^{13}C$-SOC, 5 g of sieved soil was steeped in 2 M HCl for 24 hr to remove SIC. The treated soil was washed with distilled water until the pH exceeded 5, and then it was dried at 40 °C. From each dried soil sample, approximately 30 mg soil was packed in a tin cup

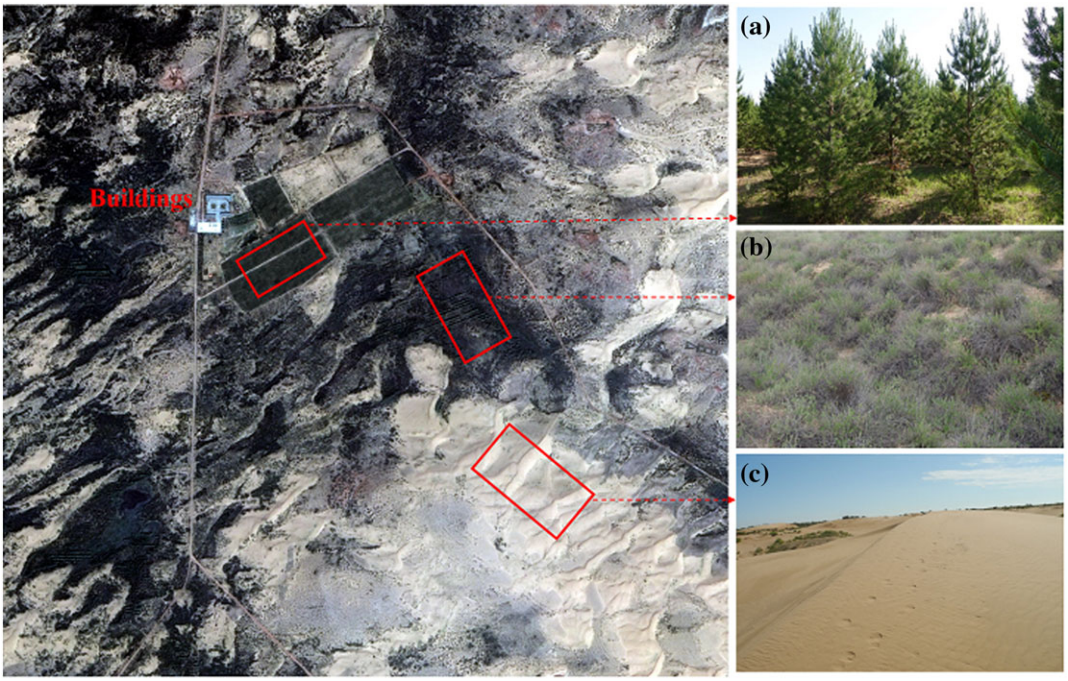

FIGURE 1 Distribution of sample plots in the study area. (a) Mongolian pine land, (b) *Artemisia ordosica* land, and (c) shifting sand land [Colour figure can be viewed at wileyonlinelibrary.com]

TABLE 1 Characteristics of the three sample plots and their soil properties (mean ± standard deviation; n = 9)

Plots	Unit	SL	MP	AO
Sample plot area	ha	8	7	5
Plant species	—	—	*Pinus sylvestris* var. *mongolica* Litv.	*Artemisia ordosica*
Stand age	year	0	10	10
Density	trees ha^{-1}	0	898 (35)	3,964 (228)
Height	m	0	6.2 (1.1)	1.1 (0.4)
DBH/ground diameter	cm	0	7.5 (1.3)	2.4 (0.5)
Coverage	%	0	61.3	87.4
$\delta^{13}C$ of leaves	‰	—	−28.06 (0.69)	−28.77 (0.85)
$\delta^{13}C$ of roots	‰	—	−27.84 (0.72)	−28.43 (0.64)
Mainly associated plants	—	—	*Agropyron cristatum*	*Setaria viridis*
Soil pH	—	8.6 (0.3)	8.3 (0.4)	8.1 (0.3)
Soil electrical conductivity	dS m^{-1}	4.75 (0.35)	4.58 (0.36)	4.62 (0.44)
Ca^{2+} in the soil	cmol kg^{-1}	5.01 (0.13)	4.62 (0.25)	4.35 (0.31)
Mg^{2+} in the soil	cmol kg^{-1}	0.55 (0.06)	0.44 (0.05)	0.38 (0.05)
Soil total porosity	%	40.2	44.5	45.2
Soil bulk density (0–20 cm)	g cm^{-3}	1.58 (0.11)	1.47 (0.14)	1.45 (0.14)
Soil bulk density (20–40 cm)	g cm^{-3}	1.56 (0.08)	1.50 (0.12)	1.46 (0.15)
Soil bulk density (40–60 cm)	g cm^{-3}	1.57 (0.04)	1.51 (0.09)	1.49 (0.12)
Soil bulk density (60–80 cm)	g cm^{-3}	1.59 (0.05)	1.55(0.11)	1.52 (0.13)
Soil bulk density (80–100 cm)	g cm^{-3}	1.57 (0.07)	1.53 (0.08)	1.55 (0.15)

Note. DBH = diameter at breast height; SL = sand land.

and analyzed with an elemental analyzer (Flash EA 1112, Thermo Fisher Scientific, Inc.) and an IRMS (Finnigan MAT Delta plus XP, Thermo Fisher Scientific, Inc.). The contents of the tin cup were combusted at 1,000 °C in the EA, and then the SOC of the sample in the tin cup was converted to CO_2. The CO_2 from the EA was ionized, and its $\delta^{13}C$ value was measured by IRMS. To determine ^{13}C-SIC, approximately 100 mg sieved soil was reacted with 5 mL 100% H_3PO_4 for 2 hr at 75 °C in a 12-mL sealed vessel of Gas Bench II (Thermo Fisher Scientific, Inc.) to generate CO_2, and the generated CO_2 was measured by IRMS (Finnigan MAT Delta plus XP, Thermo Fisher Scientific, Inc.).

The stable isotope compositions of the SOC and SIC, expressed in delta (δ) notation, were both calculated as follows (Coplen, 2011):

$$\delta^{13}C = \frac{\left(^{13}C/^{12}C\right)_{sample}}{\left(^{13}C/^{12}C\right)_{standard}} - 1, \quad (2)$$

Where: $(^{13}C/^{12}C)_{sample}$ and $(^{13}C/^{12}C)_{standard}$ are the atomic ratio of ^{13}C to ^{12}C in the sample and in the Vienna Pee Dee Belemnite standard, respectively. All samples were measured in triplicate. In the three measurements for each sample, the standard deviation of the reported $\delta^{13}C$-SOC and $\delta^{13}C$-SIC in this study was within 0.3‰ and 0.2‰, respectively.

On the basis of the transformation relationship between SOC and SIC and following Landi et al. (2003) and Wang et al. (2014), the content of PIC (g kg^{-1}) was estimated as follows:

$$\text{PIC content} = \frac{\delta^{13}C\text{-SIC} - \delta^{13}C\text{-LIC}}{\delta^{13}C\text{-PIC} - \delta^{13}C\text{-LIC}} \times \text{SIC content}, \quad (3)$$

Where: $\delta^{13}C$-SIC, $\delta^{13}C$-PIC, and $\delta^{13}C$-LIC were the stable ^{13}C of SIC, PIC, and LIC, respectively. The SIC content (g kg^{-1}) and $\delta^{13}C$-SIC have been determined in the above section. Due to lack of the specific research for desert soil, the accurate $\delta^{13}C$-LIC cannot be identified at present. It is only known that the $\delta^{13}C$-LIC of desert soil ranges from the minimum value at −2‰ to the maximum value at 2‰ (Marion et al., 1991; Ryskov et al., 2008). In this study, PIC contents were estimated using the $\delta^{13}C$-LIC values as −2‰, −1‰, 0‰, 1‰, and 2‰, respectively. On the basis of Mermut, Amundson, and Cerling (2000), $\delta^{13}C$-PIC was calculated from the $\delta^{13}C$-SOC:

$$\delta^{13}C\text{-PIC} = \delta^{13}C\text{-SOC} + 14.9‰, \quad (4)$$

Where: the value of 14.9‰ represented an average difference in stable ^{13}C composition between SOC and PIC, which included the isotopic fractionation of 4.4‰ for CO_2 diffusion and 10.5‰ for carbonate precipitation (Cerling, 1984; Cerling, Quade, Wang, & Bowman, 1989; Cerling, Solomon, Quade, & Bowman, 1991). After the estimation of PIC contents, the stocks of PIC in MP and AO lands were calculated as in Equation 1. Notably, the effect of plant on PIC is very little in the SL (almost no plant on SL), and Equation 4 is not suitable for calculating $\delta^{13}C$-PIC, so the PIC stock in SL cannot be estimated.

2.4 | Statistical analyses

The statistical analysis was performed using version 16.0 of the SPSS software (SPSS, Chicago, IL, USA). Two-way analysis of variance was carried out to test the effects of the soil depth and treatment as well as their interactions on soil carbon contents and soil $\delta^{13}C$ values (Table 2). Multiple-comparison and one-way analysis of variance

TABLE 2 Two-way analysis of variance for soil carbon contents, δ^{13}C-SIC and δ^{13}C-SOC, in different treatments and soil layers

Soil carbon	Treatment		Layer		Treatment × Layer	
	F	*p*	*F*	*p*	*F*	*p*
SOC	2,480.1	<.001	75.4	<.001	27.8	<.001
SIC	879.5	<.001	17.7	<.001	6.11	<.001
δ^{13}C-SOC	330.1	<.001	82.0	<.001	20.6	<.001
δ^{13}C-SIC	344.3	<.001	44.4	<.001	9.27	<.001

Note. SIC = soil inorganic carbon; SOC = soil organic carbon.

procedures were used to compare the differences in the soil carbon contents and soil δ^{13}C values between the different treatments within the same depth, and between different soil depths within the same treatment. Mean comparisons were performed using the least significant difference test. Linear regression analyses were carried out to evaluate the relationships between various carbon variables (δ^{13}C-SIC vs. SIC, SIC vs. SOC, and δ^{13}C-SIC vs. δ^{13}C-SOC).

3 | RESULTS

3.1 | Changes in SIC and SOC following vegetation rehabilitation

SIC contents were enhanced by vegetation rehabilitation. Within 0–100 cm depth, the SIC contents in each 20-cm depth interval in MP and AO lands were significantly higher than those in SL (Table 3). In comparison to MP land, the SIC contents in AO land exhibited considerably larger values in all five layers. Vegetation rehabilitation also elevated SIC stocks. The SIC stock at 0–100 cm in SL was 22.7 Mg ha^{-1}, and it significantly increased by 12.6 and 25.8 Mg ha^{-1} in the MP and AO lands, respectively (Figure 2a). The SIC contents in SL were almost evenly distributed among the five soil layers within a depth of 100 cm; however, this vertical distribution was altered by vegetation rehabilitation (Table 3). In AO land, the SIC contents gradually declined with depth, and significant differences existed between the two adjacent soil layers. In MP land, the SIC contents exhibited a decreasing trend with depth. The SIC content at 0–20 cm was significantly greater than that at 40–60 cm, which, in turn, was greater than that at 60–100 cm; however, no difference was observed between 20–40 and 40–60 cm or between 60–80 and 80–100 cm.

TABLE 3 Soil carbon contents in shifting sand land (SL), Mongolian pine (MP) land, and *Artemisia ordosica* (AO) land (g kg^{-1}; mean ± standard deviation; *n* = 21)

Soil carbon	Soil depth (cm)	SL	MP	AO
SIC	0–20	1.47 (0.18) Ac	2.73 (0.38) Ab	4.19 (0.57) Aa
	20–40	1.47 (0.18) Ac	2.68 (0.43) ABb	3.68 (0.57) Ba
	40–60	1.36 (0.18) Ac	2.45 (0.38) Bb	3.27 (0.43) Ca
	60–80	1.49 (0.17) Ac	1.94 (0.36) Cb	2.93 (0.63) Da
	80–100	1.43 (0.21) Ac	1.90 (0.30) Cb	2.23 (0.44) Ea
SOC	0–20	0.40 (0.02) Ac	2.83 (0.49) Ab	4.36 (0.52) Aa
	20–40	0.38 (0.02) Ac	2.14 (0.32) Bb	3.31 (0.59) Ba
	40–60	0.42 (0.04) Ac	1.74 (0.34) Cb	2.96 (0.52) Ca
	60–80	0.38 (0.04) Ac	1.76 (0.13) Cb	2.51 (0.35) Da
	80–100	0.41 (0.03) Ac	1.56 (0.22) Cb	1.87 (0.37) Ea

Note. Within each treatment, different uppercase letters denote significant differences among the depths ($p < .05$); within each depth, different lowercase letters denote significant differences among the treatments ($p < .05$). SIC = soil inorganic carbon; SOC = soil organic carbon.

The SOC content increased considerably after vegetation rehabilitation. The SOC contents in MP and AO lands showed a significant increase in each soil layer corresponding to the same depth of SL (Table 3). Compared to SL (6.2 Mg ha^{-1}), SOC stocks at 0–100 cm in MP and AO lands significantly increased by 24.0 and 38.4 Mg ha^{-1}, respectively (Figure 2b). The TSC stock within depth of 0–100 cm in SL was 28.9 Mg ha^{-1}. After vegetation rehabilitation for 10 years, the TSC stock within this depth in MP land was 65.5 Mg ha^{-1}, which was significantly lower than that in AO land (93.1 Mg ha^{-1}). Compared to those of SL, the accumulation rates of TSC at 0–100 cm in MP and AO lands were 3.7 Mg ha^{-1} yr^{-1} (or 12.7% yr^{-1}) and 6.4 Mg ha^{-1} yr^{-1} (or 22.2% yr^{-1}), respectively. Additionally, the silt and clay contents at 0–20 cm in MP and AO lands were significantly higher than those in SL. Within the depth layer of 20–100 cm, no significant difference in fine particles was observed between MP land and SL or between AO land and SL (Table 4).

3.2 | Changes in δ^{13}C-SIC and δ^{13}C-SOC following vegetation rehabilitation

δ^{13}C-SIC exhibited little variation at 0–100 cm in SL (Table 5), whereas it increased gradually with soil depth in AO and MP lands. Vegetation rehabilitation significantly reduced the δ^{13}C-SIC within 0–80 cm. In the four soil layers at 0–80 cm, the δ^{13}C-SIC values in AO land were significantly lower than those in MP land, and both of them were significantly lower than those in SL. At 80–100 cm, the δ^{13}C-SIC in AO land was significantly lower than that in SL, but no significant difference was observed between AO land and MP land or between MP land and SL.

δ^{13}C-SOC in SL land was evenly distributed among the five soil layers from 0 to 100 cm. The δ^{13}C-SOC in AO and MP lands increased gradually with soil depth (Table 5). However, no significant difference was observed between 0–20 and 20–40 cm in AO land, or between 20–40 and 40–60 cm in MP land. Vegetation rehabilitation significantly reduced δ^{13}C-SOC within depth of 0–100 cm. At all five soil layers, δ^{13}C-SOC values showed no significant difference between AO and MP lands, but these values were much lower than those in SL. The estimated PIC stocks at five layers within depth of 0–100 cm in MP and AO lands were shown in Table 6. The PIC stocks at 0–100 cm ranged from 16.2 to 26.0 Mg ha^{-1} in AO land and ranged from 9.3 to 17.3 Mg ha^{-1} in MP land (Table 6), when setting the δ^{13}C-LIC values as −2‰, −1‰, 0‰, 1‰, and 2‰, respectively.

A strong correlation between SIC content and δ^{13}C-SIC was shown in Figure 3. With the use of all 315 samples, the relationship between SIC content and δ^{13}C-SIC was fit to a linear model, and δ^{13}C-SIC explained 70% of the variation in SIC ($R^2 = .70$, $p < .01$). Additionally, our data suggested that the variations in SIC and δ^{13}C-SIC were related to SOC and δ^{13}C-SOC, respectively. The entire dataset (315 samples) exhibited positively linear relationships between SIC and SOC contents ($R^2 = .69$, $p < .01$, Figure 4a) and between δ^{13}C-SIC and δ^{13}C-SOC ($R^2 = .61$, $p < .01$, Figure 4b).

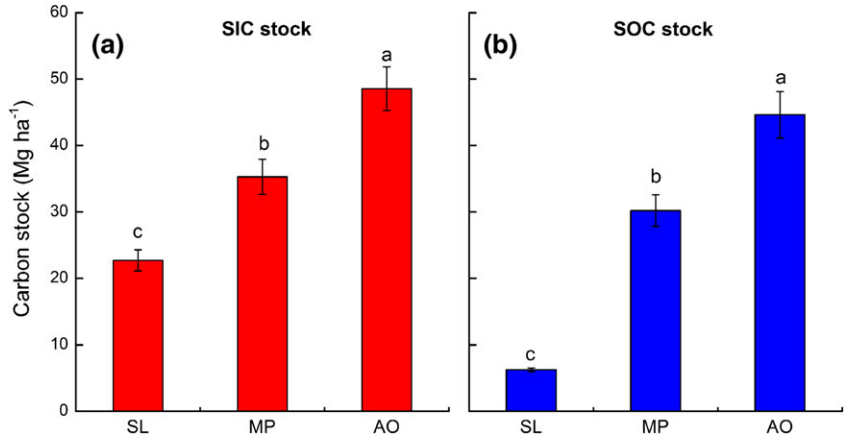

FIGURE 2 (a) Soil inorganic carbon and (b) soil organic carbon stocks within 0–100 cm under shifting sand land (SL), Mongolian pine (MP) land, and *Artemisia ordosica* (AO) land. Values with different lowercase letters are significantly different (n = 21, significance of the difference was considered as p < .05) [Colour figure can be viewed at wileyonlinelibrary.com]

TABLE 4 Soil particle size distribution in shifting sand land (SL), Mongolian pine (MP) land, and *Artemisia ordosica* (AO) land (mean ± standard deviation; n = 9)

Soil particle	Soil depth (cm)	SL	MP	AO
Sand (>0.05 mm, %)	0–20	90.8 (3.5) a	89.2 (3.9) a	88.7 (2.9) a
	20–40	91.2 (2.6) a	90.9 (2.8) a	90.8 (3.2) a
	40–60	91.2 (2.1) a	90.6 (2.1) a	91.0 (3.4) a
	60–80	91.7 (3.2) a	91.2 (3.6) a	91.1 (3.8) a
	80–100	92.1 (3.3) a	92.1 (2.7) a	92.5 (3.9) a
Silt (0.002–0.05 mm, %)	0–20	5.0 (0.3) b	5.6 (0.3) a	6.0 (0.3) a
	20–40	4.9 (0.2) a	5.1 (0.3) a	5.0 (0.5) a
	40–60	5.1 (0.3) a	5.3 (0.4) a	5.1 (0.3) a
	60–80	4.6 (0.2) a	5.0 (0.4) a	4.9 (0.3) a
	80–100	4.9 (0.4) a	4.8 (0.3) a	4.6 (0.4) a
Clay (<0.002 mm, %)	0–20	4.2 (0.4) b	5.2 (0.2) a	5.3 (0.4) a
	20–40	3.9 (0.5) a	4.0 (0.5) a	4.2 (0.3) a
	40–60	3.7 (0.6) a	4.1 (0.5) a	3.9 (0.5) a
	60–80	3.7 (0.4) a	3.8 (0.3) a	4.0 (0.4) a
	80–100	3.0 (0.5) a	3.1 (0.4) a	2.9 (0.3) a

Note. Within each depth, different lowercase letters denote significant differences among the treatments (p < .05).

4 | DISCUSSION

4.1 | Effects of vegetation rehabilitation on SIC and SOC

The SIC stocks in MP and AO lands were significantly higher than those in SL (Figure 2a). Our results were supported by those of Su et al. (2010), Li et al. (2013), and Niu, Liu, Zhao, and Qin (2015) who reported that SIC accumulation occurred following vegetation rehabilitation on SL. Nevertheless, our findings were not consistent with earlier reports of decreased or redistributed SIC following vegetation rehabilitation on the Columbia Plateau of Oregon, USA (Sartori et al., 2007), and on the Loess Plateau of China (Chang et al., 2012; Liu, Wei, Cheng, & Li, 2014). The reduction or redistribution of SIC in these previous results was primarily prompted by irrigation or surface runoff, which can remove dissolved inorganic carbon from the restored ecosystem. In this study, similar processes would not be applicable because there was no irrigation or heavy rainfall. Therefore, our findings indicated that vegetation rehabilitation on SL has a high potential to sequester SIC in semiarid deserts.

We found that plantation lands stored more SOC than SL, and the SOC stock in shrubland was significantly higher than that in forestland (Figure 2b). In the Horqin Sandy Land in China, planting shrubs also led to a more efficient SOC accumulation rate than pines afforestation (Li et al., 2013; Zhao et al., 2007). In a harsh desert environment, the increase in SOC mainly depends on the rate of fine root decomposition (Hobbie, Oleksyn, Eissenstat, & Reich, 2010). AO exhibited a faster SOC sequestration rate than did other shrubs in desert, because the rate of fine root decomposition was at least 50% faster than that of other species (Lai et al., 2016). However, the fine roots of MP contain abundant lignin and cutin (Berg & Matzner, 1997), which are difficult to decompose and transform in the short term (Novara et al., 2013). The rate of fine root decomposition for MP was likely slower than that for AO, which may result in shrubland storing more SOC than forestland in desert. After vegetation rehabilitation, the accumulation rate of TSC at

TABLE 5 δ^{13}C-SIC and δ^{13}C-SOC in shifting sand land (SL), Mongolian pine (MP) land, and *Artemisia ordosica* (AO) land (‰; mean ± standard deviation; n = 21)

	Soil depth (cm)	SL	MP	AO
δ^{13}C-SIC	0–20	−3.41 (0.23) Aa	−5.39 (0.68) Ab	−6.26 (0.43) Ac
	20–40	−3.30 (0.35) Aa	−4.91 (0.64) Bb	−5.55 (0.46) Bc
	40–60	−3.26 (0.35) Aa	−4.53 (0.58) Cb	−5.07 (0.55) Cc
	60–80	−3.29 (0.48) Aa	−3.68 (0.57) Db	−4.72 (0.56) Dc
	80–100	−3.27 (0.38) Aa	−3.51 (0.53) Dab	−3.67 (0.44) Eb
δ^{13}C-SOC	0–20	−18.40 (2.37) Aa	−29.54 (1.95) Ab	−30.37 (2.28) Ab
	20–40	−18.47 (1.25) Aa	−27.55 (2.57) Bb	−28.74 (1.92) Ab
	40–60	−18.00 (2.08) Aa	−26.58 (3.00) Bb	−25.79 (2.68) Bb
	60–80	−18.12 (1.90) Aa	−24.61 (3.08) Cb	−23.55 (2.87) Cb
	80–100	−17.93 (1.93) Aa	−22.11 (3.08) Db	−22.32 (3.09) Db

Note. Within each treatment, different uppercase letters denote significant differences among the depths (p < .05); within each depth, different lowercase letters denote significant differences among the treatments (p < .05). SIC = soil inorganic carbon; SOC = soil organic carbon.

TABLE 6 The estimated pedogenic inorganic carbon stocks in Mongolian pine (MP) land and *Artemisia ordosica* (AO) land (Mg ha^{-1}; mean ± standard deviation; n = 21)

	Soil depth (cm)	δ^{13}C-LIC				
		−2.00‰	−1.00‰	0.00‰	1.00‰	2.00‰
MP	0–20	2.15 (0.30)	2.58 (0.36)	2.95 (0.42)	3.28 (0.46)	3.56 (0.50)
	20–40	2.20 (0.35)	2.70 (0.43)	3.12 (0.50)	3.48 (0.56)	3.80 (0.61)
	40–60	1.94 (0.30)	2.45 (0.38)	2.87 (0.45)	3.23 (0.51)	3.54 (0.55)
	60–80	1.31 (0.24)	1.85 (0.34)	2.28 (0.42)	2.63 (0.49)	2.92 (0.54)
	80–100	1.68 (0.27)	2.35 (0.37)	2.83 (0.45)	3.19 (0.51)	3.48 (0.55)
	0–100	9.28 (0.70)	11.93 (0.89)	14.06 (1.05)	15.81 (1.19)	17.29 (1.30)
AO	0–20	3.85 (0.53)	4.42 (0.61)	4.92 (0.67)	5.36 (0.73)	5.75 (0.79)
	20–40	3.25 (0.50)	3.84 (0.59)	4.34 (0.67)	4.78 (0.73)	5.16 (0.79)
	40–60	3.36 (0.44)	4.01 (0.52)	4.53 (0.59)	4.97 (0.65)	5.34 (0.70)
	60–80	3.64 (0.79)	4.33 (0.93)	4.86 (1.05)	5.28 (1.14)	5.62 (1.21)
	80–100	2.13 (0.42)	2.88 (0.56)	3.42 (0.67)	3.83 (0.75)	4.16 (0.81)
	0–100	16.23 (1.11)	19.47 (1.33)	22.08 (1.51)	24.22 (1.65)	26.03 (1.77)

Note. LIC = lithogenic inorganic carbon.

0–100 cm in AO land (6.4 Mg ha^{-1} yr^{-1} or 22.2% yr^{-1}) was much higher than that in MP land (3.7 Mg ha^{-1} yr^{-1} or 12.7% yr^{-1}). AO, a typical and native shrub in desert, adapts to the climatic and edaphic conditions very well and is capable of covering large areas in relatively short time by aerial sowing. In terms of soil carbon sequestration, the contribution of shrub plantation may be more efficient than the tree plantation in semiarid areas.

4.2 | Implications of stable carbon isotopes for the reasons of SIC accumulation

To explain the reasons for SIC accumulation following vegetation rehabilitation, a traditional theory has been mentioned. Plant canopies can intercept and deposit fine particles in the wind-sand flow after vegetation rehabilitation. The sediment contains rich carbonate sources such as calcite and causes a rapid SIC accumulation in surface soil (Wang, Li, Xiao, & Pan, 2006). However, we found that this theory could not provide a complete explanation for SIC accumulation in the entire layer of 0–100 cm. Vegetation rehabilitation on SL not only elevates SIC stock in the surface soil layer but also increases levels in deeper layers (Table 3; Li et al., 2013). Nevertheless, vegetation rehabilitation enhanced fine particles only at the depth of 0–20 cm, excluding 20–100 cm (Table 4). In the deep layers (>20 cm), soil fine particles stack at an exceptionally slow rate (little change within 50 years) and contribute little to SIC sequestration (Li, Kong, Tan, & Wang, 2007). This result suggested that SIC sequestration is not exclusively derived from fine particle deposition and that other processes for SIC accumulation may be occurring after vegetation rehabilitation, which was also reflected by the stable carbon isotopes data in our study.

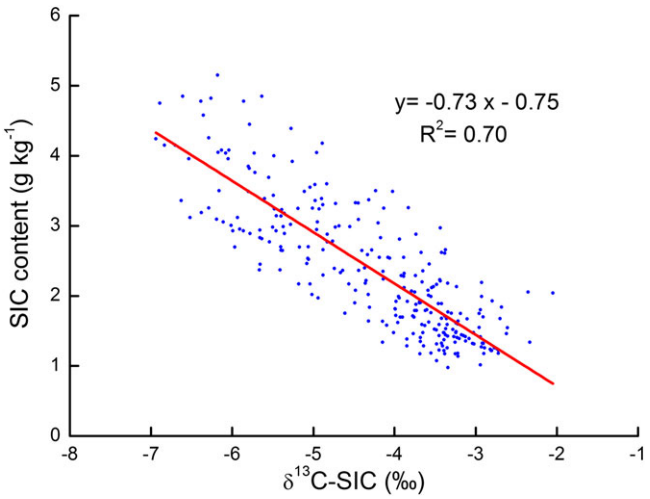

FIGURE 3 Relationship between soil inorganic carbon (SIC) content and inorganic δ^{13}C value (δ^{13}C-SIC; using all 315 samples from three sample plots). Significance of the linear regression was considered as p < .01 [Colour figure can be viewed at wileyonlinelibrary.com]

The δ^{13}C-SIC observed in SL in this study agreed with the findings in a few deserts in northwest China (Wang et al., 2014; Wang, Wang, Zhang, & Zhao, 2015), and it declined remarkably following vegetation rehabilitation (Table 5). A similar phenomenon was observed by Wang et al. (Wang, Wang, Xu, et al., 2015). The δ^{13}C-SIC can be used to differentiate between LIC and PIC, due to their distinct isotopic signatures, which are linked to trace the sources of carbonate (Bughio et al., 2016). It has been evidenced that the depleted δ^{13}C-SIC indicates the formation of PIC after changes in the land use pattern (Bughio et al., 2016; Jin et al., 2014; Liu et al., 2014; Wang et al., 2014; Wang, Wang, Xu, et al., 2015). Accordingly, the decrease in δ^{13}C-SIC in shrubland and forestland in our study (Table 5) indicated an enhancement in PIC due to vegetation rehabilitation. More importantly, a strong negatively linear relationship between δ^{13}C-SIC and SIC content (Figure 3), which was also observed by Wang et al. (Wang, Wang, Xu, et al., 2015) in the northwest China, suggested that a declining δ^{13}C-SIC is associated with SIC accumulation following vegetation rehabilitation. Namely, PIC formation is accompanied with SIC accumulation, as δ^{13}C-SIC depletion is indicative of the formation of PIC. Therefore, the carbon isotope data in this study suggest that SIC accumulation is likely caused by PIC formation after vegetation rehabilitation on SL.

Moreover, if the amount of PIC can be estimated, the results can be used to better understand the contribution of PIC to SIC sequestration. Basing on the values of δ^{13}C-SIC, δ^{13}C-PIC, δ^{13}C-LIC, and Equations 3 and 4, Wang et al. (2014) successfully estimated that the accumulation rate of PIC varied from 60 to 179 g C m^{-2} yr^{-1} in the 0–100 cm during the fertilization of loess soil. Similarly, we tried to use this method to calculate the amount of PIC in plantation lands in

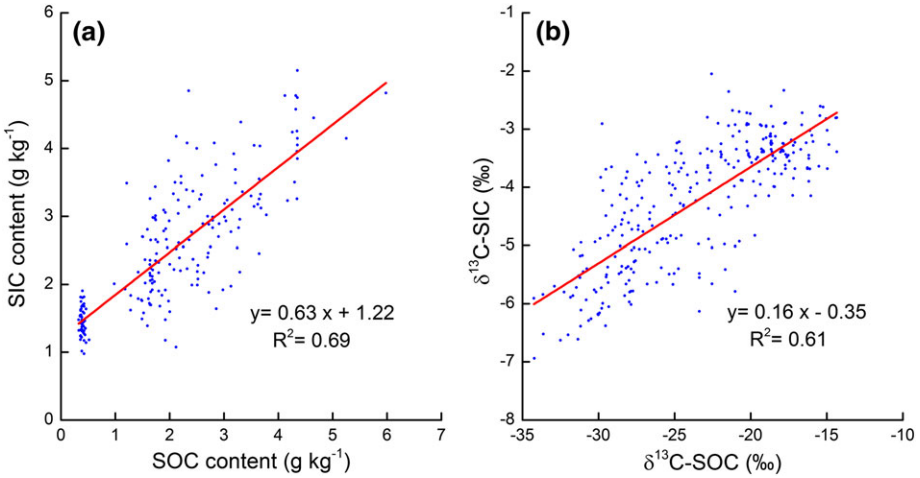

FIGURE 4 Relationships (a) between soil inorganic carbon (SIC) and organic carbon (SOC) contents and (b) between soil inorganic $\delta^{13}C$ value ($\delta^{13}C$-SIC) and soil organic $\delta^{13}C$ value ($\delta^{13}C$-SOC; using all 315 samples from three sample plots). Significance of the linear regression was considered as $p < .01$ [Colour figure can be viewed at wileyonlinelibrary.com]

our study. However, due to the lack of accurate $\delta^{13}C$-LIC data in the desert, we can only supply that the PIC stocks at 0–100 cm were approximately 9.3–17.3 Mg ha^{-1} in MP land and 16.2–26.0 Mg ha^{-1} in AO land. Interestingly, the estimated PIC stocks in plantation lands were roughly consistent with the differences in SIC stock between MP land and SL (12.6 Mg ha^{-1}), and between AO land and SL (25.8 Mg ha^{-1}; Figure 2a). The PIC stocks accounted for at least 73.8% of the increased SIC in MP land and 62.8% of the increased SIC in AO land. The results further indicated that most of the accumulated SIC following vegetation rehabilitation is likely PIC. The $\delta^{13}C$-LIC of desert soil should be precisely identified in future studies, because it is crucial for quantifying PIC stock.

4.3 | Effect of SOC accumulation on PIC formation

The positively linear relationships between the SIC and SOC contents (Figure 4a) and between $\delta^{13}C$-SIC and $\delta^{13}C$-SOC (Figure 4b) in this study were similar to the results observed in other arid regions (Landi et al., 2003; Wang, Wang, Zhang, & Zhao, 2015; Zhang, He, et al., 2010). These results implied that the PIC accumulation was closely related to the SOC accumulation following vegetation rehabilitation. Organic matter affected PIC formation by elevating soil CO_2 concentration and promoting the precipitation of carbonate in the alkaline environment (Monger et al., 2015). PIC accumulation involves two main reactions:

$$CO_2 + H_2O \leftrightarrow HCO_3^- + H^+, \quad (5)$$

$$Ca^{2+} + 2HCO_3^- \leftrightarrow CaCO_3 + H_2O + CO_2. \quad (6)$$

A mass of CO_2 was released into the soil following shrub and tree plantation in desert, mainly due to the decomposition of the increased organic matter (Zhang, Li, et al., 2013). In general, an increase in the soil CO_2 concentration would lead to the production of HCO_3^-. The accumulated HCO_3^- can drive reaction 6 to the right and result in the precipitation of carbonate (Monger et al., 2015; Wang, Wang, Zhang, & Zhao, 2015). When 2 mol of CO_2 is consumed, 1 mol of $CaCO_3$ is generated. The soil in our study site has a pH greater than 8 and is relatively rich in available Ca^{2+} and Mg^{2+} (Table 1). The decomposition of the increased SOC in the two plantation lands would dramatically elevate the soil CO_2 concentration and facilitate the occurrence of reaction 5. Under alkaline environmental conditions, the biogenic CO_2 combined with the available cations may cause continuous PIC accumulation following vegetation rehabilitation (Meyer et al., 2014; Zamanian et al., 2016).

The SIC stock in AO land was much greater than that in MP land (Figure 2a). This result was not related to the isotopic signatures of the different plant materials, because both the $\delta^{13}C$ values of roots and $\delta^{13}C$ values of leaves were not significantly different between the two species (Table 1). According to reactions 5 and 6, a high soil CO_2 concentration and soil water content can promote the precipitation of PIC and potentially lead to a difference in the SIC between AO and MP lands. Due to the stronger transpiration of trees in semi-arid areas, forestland always has lower soil water content than shrubland (Gao, Wu, Zhao, Wang, & Shi, 2014; Wang, Zeng, Chen, Zeng, & Fang, 2013). Shrubland stored more SOC than did forestland in our study site (Figure 2b), and shrubland generally displayed a higher soil respiration rate than did young pine land (Law et al., 2001; Wang et al., 2013). The high soil water content and soil respiration rate in shrubland compared to those in forestland always generate more HCO_3^-, which may cause more PIC precipitation in shrubland. Additionally, the SIC contents of plantation lands exhibited a decreasing trend along the vertical profile in this study and in other similar studies (Li et al., 2013), and this trend may be related to the process of PIC formation. Our results showed that the SOC contents sharply decreased with soil layer in AO and MP lands (Table 2). This result implied that shallow soil with a high SOC content may supply more sufficient CO_2 resource than did deep soil, when PIC precipitates. Furthermore, soil moisture decreased with the depth in the desert plantation areas (Li, Ma, Xiao, Wang, & Kim, 2004), which suggested that shallow soil with a high water content is preferable for PIC formation compared to deep soil. The above two factors may cause SIC contents to

decrease with the depth in plantation lands. However, additional studies are still needed to determine the detailed mechanisms associated with the effects of land use on carbonate stratification in arid and semiarid areas.

5 | CONCLUSION

Our results demonstrated that vegetation rehabilitation on SL has a high potential to sequester SIC and SOC in semiarid deserts. The reduction in δ^{13}C-SIC following vegetation rehabilitation indicated the formation of PIC. The negatively linear relationship between SIC content and δ^{13}C-SIC suggested that SIC sequestration is likely caused by PIC formation. The positively linear relationships between SIC content and SOC content and between δ^{13}C-SIC and δ^{13}C-SOC implied that the PIC formation may be closely related to the SOC accumulation. Our findings suggest that SIC plays an important role in the carbon cycle of desert ecosystem, and overlooking this role may lead to a substantial underestimation of the capacity for carbon sequestration following vegetation rehabilitation. The stable carbon isotope data collected in this study will help to characterize the mechanisms of SIC formation and transformation in arid and semiarid areas.

ACKNOWLEDGEMENTS

This research was supported by the National Natural Science Foundation of China (31500585). The authors thank Weiwei She, Zhen Liu, Yuxuan Bai, and Shijun Liu for their help on sample collection.

ORCID

Jiabin Liu http://orcid.org/0000-0001-5070-2906

REFERENCES

Berg, B., & Matzner, E. (1997). Effect of N deposition on decomposition of plant litter and soil organic matter in forest systems. *Environmental Reviews*, *5*(1), 1–25. https://doi.org/10.1139/a96-017

Bughio, M. A., Wang, P. L., Meng, F. Q., Qing, C., Kuzyakov, Y., Wang, X. J., & Junejo, S. A. (2016). Neoformation of pedogenic carbonates by irrigation and fertilization and their contribution to carbon sequestration in soil. *Geoderma*, *262*, 12–19. https://doi.org/10.1016/j.geoderma.2015.08.003

Cerling, T. E. (1984). The stable isotope composition of modern soil carbonate and its relationship to climate. *Earth and Planetary Science Letters*, *71*, 229–240. https://doi.org/10.1016/0012-821X(84)90089-X

Cerling, T. E., Quade, J., Wang, Y., & Bowman, J. R. (1989). Carbon isotopes in soils and paleosols as ecology and paleoecology indicators. *Nature*, *341*, 138–139. https://doi.org/10.1038/341138a0

Cerling, T. E., Solomon, D. K., Quade, J., & Bowman, J. R. (1991). On the isotopic composition of carbon in soil carbon dioxide. *Geochimica et Cosmochimica Acta*, *55*, 3403–3405. https://doi.org/10.1016/0016-7037(91)90498-T

Chang, R. Y., Fu, B. J., Liu, G. B., Wang, S., & Yao, X. L. (2012). The effects of afforestation on soil organic and inorganic carbon: A case study of the Loess Plateau of China. *Catena*, *95*, 145–152. https://doi.org/10.1016/j.catena.2012.02.012

Chaplot, V., Dlamini, P., & Chivenge, P. (2016). Potential of grassland rehabilitation through high density-short duration grazing to sequester atmospheric carbon. *Geoderma*, *271*, 10–17. https://doi.org/10.1016/j.geoderma.2016.02.010

Chen, X. H., Duan, Z. H., & Tan, M. L. (2016). Restoration affect soil organic carbon and nutrients in different particle-size fractions. *Land Degradation & Development*, *27*, 561–572. https://doi.org/10.1002/ldr.2400

Coplen, T. B. (2011). Guidelines and recommended terms for expression of stable-isotope-ratio and gas-ratio measurement results. *Rapid Communications in Mass Spectrometry*, *25*, 2538–2560. https://doi.org/10.1002/rcm.5129

Diaz-Hernández, J. L., Fernández, E. B., & González, J. L. (2003). Organic and inorganic carbon in soils of semiarid regions: A case study from the Guadix–Baza basin (Southeast Spain). *Geoderma*, *114*, 65–80. https://doi.org/10.1016/S0016-7061(02)00342-7

Easdale, M. H. (2016). Zero net livelihood degradation—The quest for a multidimensional protocol to combat desertification. *Soil*, *2*, 129–134. https://doi.org/10.5194/soil-2-129-2016

Emmerich, W. E. (2003). Carbon dioxide fluxes in a semiarid environment with high carbonate soils. *Agricultural and Forest Meteorology*, *116*, 91–102. https://doi.org/10.1016/S0168-1923(02)00231-9

FAO (FAO/IUSS Working Group WRB), 2006. *World reference base for soil resources 2006, first update 2006*. World Soil Resources Reports No, 103. FAO, Rome.

Gao, X., Wu, P., Zhao, X., Wang, J., & Shi, Y. (2014). Effects of land use on soil moisture variations in a semi-arid catchment: Implications for land and agricultural water management. *Land Degradation & Development*, *25*, 163–172. https://doi.org/10.1002/ldr.1156

Hobbie, S. E., Oleksyn, J., Eissenstat, D. M., & Reich, P. B. (2010). Fine root decomposition rates do not mirror those of leaf litter among temperate tree species. *Oecologia*, *162*, 505–513. https://doi.org/10.1007/s00442-009-1479-6

Huang, G., Zhao, X. Y., Li, Y. Q., & Cui, J. Y. (2012). Restoration of shrub communities elevates organic carbon in arid soils of northwestern China. *Soil Biology & Biochemistry*, *47*, 123–132. https://doi.org/10.1016/j.soilbio.2011.12.025

Jin, Z., Dong, Y. S., Wang, Y. Q., Wei, X. R., Wang, Y. F., Cui, B. L., & Zhou, W. J. (2014). Natural vegetation restoration is more beneficial to soil surface organic and inorganic carbon sequestration than tree plantation on the Loess Plateau of China. *Science of the Total Environment*, *485-486*, 615–623. https://doi.org/10.1016/j.scitotenv.2014.03.105

Lai, Z. R., Zhang, Y. Q., Liu, J. B., Wu, B., Qin, S. G., & Fa, K. Y. (2016). Fine-root distribution, production, decomposition, and effect on soil organic carbon of three revegetation shrub species in northwest China. *Forest Ecology and Management*, *359*, 381–388. https://doi.org/10.1016/j.foreco.2015.04.025

Lal, R. (2001). Potential of desertification control to sequester carbon and mitigate the greenhouse effect. *Climatic Change*, *51*, 35–72. https://doi.org/10.1023/A:1017529816140

Lal, R. (2004). Carbon sequestration in dryland ecosystems. *Environmental Management*, *33*, 528–544. https://doi.org/10.1007/s00267-003-9110-9

Lal, R. (2009). Sequestering carbon in soils of arid ecosystems. *Land Degradation and Development*, *20*, 441–454. https://doi.org/10.1002/ldr.934

Landi, A., Mermut, A. R., & Anderson, D. W. (2003). Origin and rate of pedogenic carbonate accumulation in Saskatchewan soils, Canada. *Geoderma*, *117*, 143–156. https://doi.org/10.1016/S0016-7061(03)00161-7

Law, B. E., Kelliher, F. M., Baldocchi, D. D., Anthoni, P. M., Irvine, J., Moore, D., & Tuyl, S. V. (2001). Spatial and temporal variation in respiration in a young ponderosa pine forest during a summer drought. *Agricultural and Forest Meteorology*, *110*, 27–43. https://doi.org/10.1016/S0168-1923(01)00279-9

Li, Y. Q., Awada, T., Zhou, X. H., Shang, W., Chen, Y. P., Zou, X. A., … Feng, J. (2012). Mongolian pine plantations enhance soil physico-chemical properties and carbon and nitrogen capacities in semi-arid degraded sandy land in China. *Applied Soil Ecology*, *56*, 1–9. https://doi.org/10.1016/j.apsoil.2012.01.007

Li, Y. Q., Brandle, J., Awada, T., Chen, Y. P., Han, J. J., Zhang, F. X., & Luo, Y. Q. (2013). Accumulation of carbon and nitrogen in the plant–soil system after afforestation of active sand dunes in China's Horqin Sandy

Land. *Agriculture, Ecosystems & Environment*, *177*, 75–84. https://doi.org/10.1016/j.agee.2013.06.007

Li, X. R., Kong, D. S., Tan, H. J., & Wang, X. P. (2007). Changes in soil and vegetation following stabilisation of dunes in the southeastern fringe of the Tengger Desert, China. *Plant and Soil*, *300*, 221–231. https://doi.org/10.1007/s11104-007-9407-1

Li, X. R., Ma, F. Y., Xiao, H. L., Wang, X. P., & Kim, K. C. (2004). Long-term effects of revegetation on soil water content of sand dunes in arid region of northern China. *Journal of Arid Environments*, *57*, 1–16. https://doi.org/10.1016/S0140-1963(03)00089-2

Li, C. F., Zhang, C., Luo, G. P., Chen, X., Maisupova, B., Madaminov, A. A., … Djenbaev, B. M. (2015). Carbon stock and its responses to climate change in Central Asia. *Global Change Biology*, *21*(5), 1951–1967. https://doi.org/10.1111/gcb.12846

Liu, W. G., Wei, J., Cheng, J. M., & Li, W. J. (2014). Profile distribution of soil inorganic carbon along a chronosequence of grassland restoration on a 22-year scale in the Chinese Loess Plateau. *Catena*, *121*, 321–329. https://doi.org/10.1016/j.catena.2014.05.019

Marion, G. M., Introne, D. S., & Cleve, K. V. (1991). The stable isotope geochemistry of $CaCO_3$ on the Tanana River floodplain of interior Alaska, USA: Composition and mechanisms of formation. *Chemical Geology: Isotope Geoscience*, *86*, 97–110. https://doi.org/10.1016/0168-9622(91)90056-3

Mermut, A. R., Amundson, R., & Cerling, T. E. (2000). The use of stable isotopes in studying carbonate dynamics in soils. In R. Lal, J. M. Kimble, H. Eswarian, & B. A. Stewart (Eds.), *Global climate change and pedogenic carbonates* (pp. 65–85). Boca Raton: CRC Press.

Meyer, N. A., Breecker, D. O., Young, M. H., & Litvak, M. E. (2014). Simulating the effect of vegetation in formation of pedogenic carbonate. *Soil Science Society of America Journal*, *78*(3), 914–924. https://doi.org/10.2136/sssaj2013.08.0326

Monger, H. C., Kraimer, R. A., Khresat, S., Cole, D. R., Wang, X. J., & Wang, J. P. (2015). Sequestration of inorganic carbon in soil and groundwater. *Geology*, *43*(5), 375–378. https://doi.org/10.1130/G36449.1

Niu, R. X., Liu, J. L., Zhao, X. Y., & Qin, Y. (2015). Ecological benefit of different revegetated covers in the middle of Hexi corridor, northwestern China. *Environmental Earth Sciences*, *74*, 5699–5710. https://doi.org/10.1007/s12665-015-4587-0

Novara, A., Gristina, L., Mantia, T. L., & Rühl, J. (2013). Carbon dynamics of soil organic matter in bulk soil and aggregate fraction during secondary succession in a Mediterranean environment. *Geoderma*, *193-194*, 213–221. https://doi.org/10.1016/j.geoderma.2012.08.036

Ryskov, Y. G., Demkin, V. A., Oleynik, S. A., & Ryskova, E. A. (2008). Dynamics of pedogenic carbonate for the last 5000 years and its role as a buffer reservoir for atmospheric carbon dioxide in soils of Russia. *Global and Planetary Change*, *61*, 63–69. https://doi.org/10.1016/j.gloplacha.2007.08.006

Sartori, F., Lal, R., Ebinger, M. H., & Eaton, J. A. (2007). Changes in soil carbon and nutrient pools along a chronosequence of poplar plantations in the Columbia Plateau, Oregon, USA. *Agriculture, Ecosystems & Environment*, *122*, 325–339. https://doi.org/10.1016/j.agee.2007.01.026

Stevenson, B. A., Kelly, E. F., McDonald, E. V., & Busacca, A. J. (2005). The stable carbon isotope composition of soil organic carbon and pedogenic carbonates along a bioclimatic gradient in the Palouse region, Washington State, USA. *Geoderma*, *124*, 37–47. https://doi.org/10.1016/j.geoderma.2004.03.006

Su, Y. Z., Wang, X. F., Yang, R., & Lee, J. (2010). Effects of sandy desertified land rehabilitation on soil carbon sequestration and aggregation in an arid region in China. *Journal of Environmental Management*, *91*, 2109–2116. https://doi.org/10.1016/j.jenvman.2009.12.014

Tan, W. F., Zhang, R., Cao, H., Huang, C. Q., Yang, Q. K., Wang, M. K., & Koopal, L. K. (2014). Soil inorganic carbon stock under different soil types and land uses on the Loess Plateau region of China. *Catena*, *121*, 22–30. https://doi.org/10.1016/j.catena.2014.04.014

Walkley, A. J., & Black, I. A. (1934). An examination of the Degtjareff method for determining soil organic matter and a proposed modification of the chromic acid titration method. *Soil Science*, *37*, 29–38. https://doi.org/10.1097/00010694-193401000-00003

Wang, X. P., Li, X. R., Xiao, H. L., & Pan, Y. X. (2006). Evolutionary characteristics of the artificially revegetated shrub ecosystem in the Tengger Desert, northern China. *Ecological Research*, *21*, 415–424. https://doi.org/10.1007/s11284-005-0135-9

Wang, K. B., Ren, Z. P., Deng, L., Zhou, Z. C., Shangguan, Z. P., Shi, W. Y., & Chen, Y. P. (2016). Profile distributions and controls of soil inorganic carbon along a 150-year natural vegetation restoration chronosequence. *Soil Science Society of America Journal*, *80*, 193–202. https://doi.org/10.2136/sssaj2015.08.0296

Wang, X. J., Wang, J. P., Xu, M. G., Zhang, W. J., Fan, T. L., & Zhang, J. (2015). Carbon accumulation in arid croplands of northwest China: Pedogenic carbonate exceeding organic carbon. *Scientific Reports*, *5*, 11439. https://doi.org/10.1038/srep11439

Wang, J. P., Wang, X. J., Zhang, J., & Zhao, C. Y. (2015). Soil organic and inorganic carbon and stable carbon isotopes in the Yanqi Basin of northwestern China. *European Journal of Soil Science*, *66*, 95–103. https://doi.org/10.1111/ejss.12188

Wang, X. J., Xu, M. G., Wang, J. P., Zhang, W. J., Yang, X. Y., Huang, S. M., & Liu, H. (2014). Fertilization enhancing carbon sequestration as carbonate in arid cropland: Assessments of long-term experiments in northern China. *Plant and Soil*, *380*, 89–100. https://doi.org/10.1007/s11104-014-2077-x

Wang, W., Zeng, W., Chen, W., Zeng, H., & Fang, J. (2013). Soil respiration and organic carbon dynamics with grassland conversions to woodlands in temperate China. *PLoS One*, *8*(8). e71986. DOI: https://doi.org/10.1371/journal.pone.0071986

Yu, Y., & Jia, Z. Q. (2014). Changes in soil organic carbon and nitrogen capacities of *Salix cheilophila* Schneid. Along a revegetation chronosequence in semi-arid degraded sandy land of the Gonghe Basin, Tibet Plateau. *Solid Earth*, *5*, 1045–1054. https://doi.org/10.5194/se-5-1045-2014

Zamanian, K., Pustovoytov, K., & Kuzyakov, Y. (2016). Pedogenic carbonates: Forms and formation processes. *Earth-Science Reviews*, *157*, 1–17. https://doi.org/10.1016/j.earscirev.2016.03.003

Zhang, Y., Cao, C. Y., Han, X. S., & Jiang, S. Y. (2013). Soil nutrient and microbiological property recoveries via native shrub and semi-shrub plantations on moving sand dunes in Northeast China. *Ecological Engineering*, *53*, 1–5. https://doi.org/10.1016/j.ecoleng.2013.01.012

Zhang, K., Dang, H., Tan, S., Cheng, X., & Zhang, Q. (2010). Change in soil organic carbon following the 'Grain-For-Green' programme in China. *Land Degradation & Development*, *21*, 13–23. https://doi.org/10.1002/ldr.954

Zhang, N., He, X. D., Gao, Y. B., Li, Y. H., Wang, H. T., Ma, D., … Yang, S. (2010). Pedogenic carbonate and soil dehydrogenase activity in response to soil organic matter in *Artemisia ordosica* community. *Pedosphere*, *20*, 229–235. https://doi.org/10.1016/S1002-0160(10)60010-0

Zhang, Z. S., Li, X. R., Nowak, R. S., Wu, P., Gao, Y. H., Zhao, Y., … Jia, R. L. (2013). Effect of sand-stabilizing shrubs on soil respiration in a temperate desert. *Plant and Soil*, *367*, 449–463. https://doi.org/10.1007/s11104-012-1465-3

Zhao, H. L., Zhou, R. L., Su, Y. Z., Zhang, H., Zhao, L. Y., & Drake, S. (2007). Shrub facilitation of desert land restoration in the Horqin Sand Land of Inner Mongolia. *Ecological Engineering*, *31*, 1–8. https://doi.org/10.1016/j.ecoleng.2007.04.010

How to cite this article: Gao Y, Dang P, Zhao Q, Liu J, Liu J. Effects of vegetation rehabilitation on soil organic and inorganic carbon stocks in the Mu Us Desert, northwest China. *Land Degrad Develop*. 2018;29:1031–1040. https://doi.org/10.1002/ldr.2832